

Random matrix theory of proximity effect in disordered wires

M. Titov and H. Schomerus

Max-Planck-Institut für Physik komplexer Systeme, Nöthnitzer Str. 38, 01187 Dresden, Germany
(August 6, 2002)

We study analytically the local density of states (LDOS) in a disordered normal-metal wire (N) at ballistic distance to a superconductor (S). Our calculation is based on a scattering-matrix approach, which concerns for wave-function localisation in the normal metal, and extends beyond the conventional semiclassical theory based on Usadel and Eilenberger equations. We also analyse how a finite transparency of the NS interface modifies the spectral proximity effect.

PACS numbers: 74.50.+r, 74.80.Fp, 73.20.Fz

I. INTRODUCTION

It is widely acknowledged that a piece of a normal metal that is in good contact with a superconductor acquires some superconducting properties. This phenomenon, named the proximity effect, has already been studied by Cooper¹ in the early sixties. Since then many theoretical and experimental investigations have been carried out.² Much owed to the recent progress in the fabrication technology of nanostructures there is a revived interest to the proximity effect in the last decade.³ One remarkable evidence of this effect is the formation of a spectral gap in the normal metal, which strongly affects the low-temperature transport properties of the normal-metal superconductor (NS) junctions. The key mechanism responsible for the appearance of the gap is the Andreev reflection at the NS boundary, which converts the dissipative electrical current into dissipationless supercurrent.⁴ Similar mechanisms act in superconductor ferromagnet junctions which have become an object of intense study recently.^{5,6} Despite the spectral gap a normal metal wire connected to a single superconductor remains resistive. This is because the size of the gap is strongly suppressed when the distance to the NS boundary increases. An effective experimental technique which allows for spatially resolved measurements of the electronic density in the nanostructures is the scanning tunnelling microscopy. It provides both a unique sub-meV energy sensitivity and an atomic spatial resolution. Several recent measurements of the local electronic density of states (LDOS) in the NS junctions^{7–11} turned out to be in very good agreement with the predictions of quasiclassical theory^{13–15} of “non-equilibrium” superconductivity, based on the Usadel equation for the diffusive transport and the Eilenberger equation for the ballistic transport.^{16,17}

The interplay of ballistic and diffusive transport becomes important when one studies local properties at short distance to an NS interface in a disordered system. Quasiparticles are then transferred to the interface by ballistic transport, while they explore the rest of the system diffusively. This situation is not covered by conventional quasiclassical theory. Quasiclassics also cannot account for the non-perturbative effects of wave-function localisation, which only can be included by a fully phase-

coherent approach.

In this paper we present a theory that goes beyond the quasiclassical description and apply it to calculate the local density of states in a NS wire geometry near the interface, at zero temperature and vanishing magnetic field.

In our model the normal metal is shaped in the form of the long disordered quantum wire, which supports N propagating modes at the Fermi level E_F . The elastic scattering mean free path ℓ in the wire is assumed to be much larger than the Fermi wave length λ_F , which corresponds to the weak disorder. The superconductor is assumed to be clean and characterised by the bulk value Δ of the amplitude of the pair potential. The superconductor order parameter is assumed to be constant Δ in the superconductor and zero in the normal metal. Throughout the paper we disregard the suppression of the pair potential in the superconductor on approaching the NS interface, which might play an essential role for energies close to Δ . This approximation is referred to in the literature as a “rigid boundary condition”.¹⁸

We calculate the mean LDOS, or, more precisely, its envelope, at a distance x on the normal-metal side of the NS interface as shown schematically in Fig. 1. The envelope is obtained by averaging the LDOS over distances of the order of the Fermi wave length λ_F . The spatial averaging smears out the Friedel type oscillations and makes the LDOS independent on the position across the wire. We study in detail the case that the distance x is small compared to the scattering mean free path ℓ , so that $\lambda_F \ll x \ll \ell$, while the ratio between the superconductor coherence length $\xi = \hbar v_F / \Delta$ and ℓ remains arbitrary. The resulting mean LDOS found by averaging over disorder does not depend on x and is a smooth function of energy everywhere except at $\varepsilon = \Delta$ (the energy ε is measured from the Fermi surface).

Our calculation is organised as follows. In Section II we derive a general relation between the one-point Green function in a quantum wire and the reflection matrices r_L, r_R . These matrices relate the plane-wave components of the quasiparticle wave function in the process of reflection from the parts of the wire to the left and to the right part of x .

We apply this result in Section III in order to calculate the mean LDOS in the neighbourhood of an ideally

transmitting NS interface. The matrices r_L , r_R of the size $2N \times 2N$ describe the reflection of the electron- and hole-like quasiparticles. The left reflection matrix r_L is diagonal in the electron-hole representation and depends on the disorder in the normal metal. The right reflection matrix r_R is off-diagonal (in absence of the tunnel barrier) and is fixed within the model considered.

In the region $\varepsilon < \Delta$ we obtain the disorder-averaged LDOS

$$\bar{n}(x, \varepsilon) = \pi \rho_\varepsilon(\phi_A), \quad \phi_A = \arccos \varepsilon / \Delta, \quad (1)$$

where the function $\rho_\varepsilon(\phi)$ is the probability density of the eigenphase of the matrix correlator $r_0(\varepsilon)r_0(-\varepsilon)^\dagger$. The reflection matrix $r_0(\varepsilon)$ relates the plane-wave amplitudes of the electron wave function in the process of reflection from the semi-infinite normal-metal wire. The probability density $\rho_\varepsilon(\phi)$ has been studied in Ref. 19. Apart from energy and phase it depends on the number of channels N and the mean scattering time $\tau_s = \ell/v_F$. According to Ref. 19 one can distinguish localised, diffusive and ballistic regimes in the form of the function $\rho_\varepsilon(\phi)$ depending on the value of ε . We observe the effect of Anderson localisation in the linear increase of the LDOS for energies smaller than the Thouless energy $\varepsilon_c = \hbar/N^2\tau_s$. We also find that the curves calculated for different number of channels in the wire are lying close to each other at any ratio ℓ/ξ (see Fig. 2). This suggests that the weak-localisation correction to the LDOS is small in the case of the ideally transmitting NS interface.

In Section IV we generalise the model to include a tunnel barrier at the interface, parametrised by a tunnel probability per mode Γ . We calculate analytically the LDOS near the interface in the extreme cases of a localised wire, $N = 1$, and a diffusive wire, $N \gg 1$.

The effect of the tunnel barrier consists of a reduction of the pseudogap in the normal metal. This effect is most pronounced in the dirty regime $\ell \lesssim \xi$, or $\Delta\tau_s/\hbar \lesssim 1$. The results of our calculation for the diffusive wire in the intermediate regime $\ell = \xi$ are summarised in Fig. 5 for different values of Γ . We observe that the LDOS increases monotonously to its bulk constant value around the energy $\hbar\Gamma^2/\tau_s$ and reveals a high and narrow peak close to $\varepsilon = \Delta$.

The monotonous reduction of the pseudogap is attributed to the quasiparticles which experience normal reflection at the tunnel barrier and therefore do not see the NS boundary. The formation of the peak is due to the quasiparticles reflected from the superconductor.

When the distance x increases beyond the mean free path ℓ a competing effect takes place. That is the suppression of the pseudogap due to the back-scattering on the weak disorder potential in the normal-metal segment of length x in front of the interface. The estimated size of the pseudogap due to this effect is $\hbar D/x^2$, where $D = v_F\ell$ is the diffusion constant in the normal metal. In this case the LDOS considerably overshoots its bulk value around $\varepsilon = \hbar D/x^2$, which is in contrast to the monotonous increase due to the tunnelling into the superconductor. We

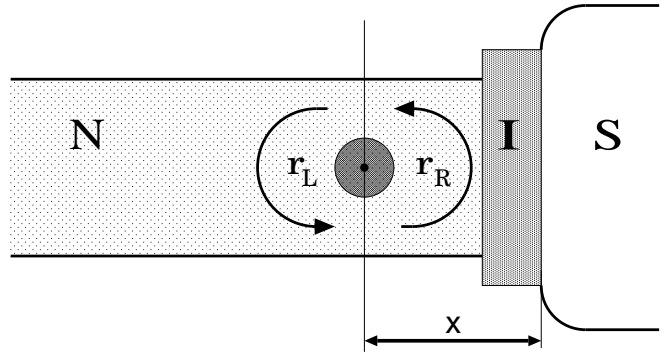


FIG. 1. The geometry of the NS junction consisting of a long normal-metal disordered wire N, a clean superconductor S and a dielectric tunnel barrier I in between. The envelope of the mean local density of states (LDOS) is calculated at the distance x from the NS interface, with $\lambda_F \ll x \ll \ell$. The envelope is obtained by spatial averaging the LDOS over an area (dark circle) with size of the order of the Fermi wave length λ_F . The matrix r_L relates the plane-wave components in the process of reflection from the normal-metal disordered wire. The matrix r_R describes the reflection from the tunnel barrier – superconductor part of the junction. The mean LDOS is found by averaging over the disorder-induced fluctuations of the matrix r_L .

therefore anticipate that the effect of the tunnel barrier still can be seen in the shape of the LDOS provided $\hbar D/x^2 \gg \hbar\Gamma^2/\tau_s$, or equivalently $x \ll \ell/\Gamma$. Namely, at distances smaller than ℓ/Γ the LDOS may acquire the step-like feature at the value $\varepsilon = \hbar\Gamma^2/\tau_s$, which is fixed by the NS interface transparency rather than by the distance to the interface.

A qualitatively similar phenomenon has been indeed observed in experiments by Levi *et. al.*¹¹ in the Cu barrier pin wires near a N(Cu)-S(NbTi) boundary.

On contrary, at large distances $x \gg \ell/\Gamma$ the barrier is not effective in the sense that its presence cannot be distinguished in the energy dependence of the LDOS. This is consistent with a general semiclassical criterion¹² which states that the barrier is not effective for a given observable if the most of the relevant trajectories hit the NS interface more than Γ^{-1} times before the electron-hole coherence is lost. In the case of the LDOS this criterion is fulfilled for $x \gg \ell/\Gamma$.

The tunnel barrier acts differently for the single-channel wire. In the dirty regime $\ell \lesssim \xi$ the size of the pseudogap $\hbar\Gamma/\tau_s$ scales linearly with Γ due to the Anderson localisation. This results in a different shape of the LDOS compared to the diffusive case ($N \gg 1$). The difference becomes more and more pronounced with decreasing ratio ℓ/ξ or tunnelling probability Γ .

II. GREEN FUNCTION IN A WIRE GEOMETRY

In our model of the NS junction the normal metal is shaped in the form of a semi-infinite quasi-one dimensional disordered wire. The properties of such a system is well understood in the framework of the scattering theory²⁰ provided the weak disorder limit $\lambda_F \ll \ell$. The detailed statistical description of the disorder scattering is based on the Dorokhov-Mello-Pereyra-Kumar (DMPK) equation.^{21,22} This is a scaling equation for the probability distribution of the scattering matrix of a segment of the wire. Below we derive a general relation between the one-point Green function and the reflection matrices r_L , r_R for two parts of the wire. The single-channel counterpart of this relation has been used recently to reconsider the problem of LDOS fluctuations in 1D normal-metal wires.²³

The disordered wire has the Hamiltonian $H = H_0 + V(\vec{r})$, where $V(\vec{r})$ is a disordered potential. We parametrise $\vec{r} = (x, \vec{\rho})$, where x is the coordinate along the wire and $\vec{\rho}$ is the vector in the transversal direction. We first discuss the case of ‘spinless’ electrons, assuming $H_0 = -\frac{1}{2m_e}\nabla^2$, $\hbar = 1$, and include hole-like quasiparticles in Sections III and IV.

In the absence of V the quantisation in the transversal direction gives rise to a set of N propagating modes characterised by the transverse momentum \vec{q}_n . The total energy $E = (1/2m_e)(|\vec{q}_n|^2 + k_n^2)$, where the x -momentum k_n is conserved. The retarded Green function $G^R(E) = (E + i\eta - H)^{-1}$ is written in the channel representation as

$$G_{nm}^R(x, x') = \iint_A d\vec{\rho} d\vec{\rho}' \langle n | \vec{\rho} \rangle \langle \vec{\rho}' | m \rangle \langle \vec{r} | G^R | \vec{r}' \rangle, \quad (2)$$

where the integration is carried out over a cross-sectional area A . Hence the LDOS

$$n(\vec{r}, \varepsilon) = -\frac{1}{\pi} \text{Im} \sum_{n,m} \langle m | \vec{\rho} \rangle \langle \vec{\rho} | n \rangle G_{nm}^R(x, x), \quad (3)$$

where ε is the energy measured from the Fermi surface. For a two-dimensional wire of the width d we have $\langle \rho | n \rangle = (2/d)^{1/2} \sin(\pi n \rho / d)$. In what follows we shall omit the index R , assuming everywhere the retarded Green function.

Let us formally cut the wire in the point x into two pieces and treat the left and the right part separately. We decompose the potential $V = V_R + V_L$, where $V_{R,L}$ is the disorder potential in the right and the left part of the wire, respectively. We also introduce the left and the right Green function as $G_{R,L} = (E + i\eta - H_0 - V_{L,R})^{-1}$. According to Fisher and Lee, Ref. 24, we have

$$G_{L,R;nm}(x, x) = \frac{1}{i\sqrt{v_n v_m}} (\delta_{nm} + r_{L,R;nm}(x)), \quad (4)$$

where $v_n = k_n/m_e$ is the channel velocity and $r_{L,R}$ are the reflection matrices from the left and the right part of the wire, respectively.

The Green functions obey Dyson equations which can be written in the matrix form as

$$\hat{G}(x, x) = \hat{G}_0(x, x) + \int_{-\infty}^{\infty} dy \hat{G}_0(x, y) \hat{V}(y) \hat{G}(y, x), \quad (5a)$$

$$\hat{G}(x, x) = \hat{G}_R(x, x) + \int_{-\infty}^x dy \hat{G}_R(x, y) \hat{V}_L(y) \hat{G}(y, x), \quad (5b)$$

$$\hat{G}(x, x) = \hat{G}_L(x, x) + \int_x^{\infty} dy \hat{G}_L(x, y) \hat{V}_R(y) \hat{G}(y, x), \quad (5c)$$

where the elements of the matrix \hat{V} are given by

$$V_{nm}(x) = \int_A d\vec{\rho} \langle n | \vec{\rho} \rangle \langle \vec{\rho} | m \rangle V(\vec{r}), \quad (6)$$

and the ballistic Green function (in absence of the potential) reads

$$G_{0,nm}(x, x') = \frac{\delta_{nm}}{iv_n} e^{ik_n|x-x'|}. \quad (7)$$

We also take advantage of the following relations²⁵

$$G_{R,nl}(x, y) = e^{-ik_l(x-y)} G_{R,nl}(x, x), \quad \text{for } y < x, \quad (8a)$$

$$G_{L,nl}(x, y) = e^{-ik_l(x-y)} G_{L,nl}(x, x), \quad \text{for } y > x, \quad (8b)$$

in the disorder-free regions in order to eliminate the integral terms in Eq. (5). As a result we obtain the matrix equality

$$\frac{1}{\hat{G}(x, x)} + \frac{1}{\hat{G}_0(x, x)} = \frac{1}{\hat{G}_R(x, x)} + \frac{1}{\hat{G}_L(x, x)}. \quad (9)$$

Using Eqs. (4) and (7) we finally get

$$\hat{G}(x, x) = \frac{1}{\sqrt{i\hat{v}}} (1 + \hat{r}_R) \frac{1}{1 - \hat{r}_L \hat{r}_R} (1 + \hat{r}_L) \frac{1}{\sqrt{i\hat{v}}}, \quad (10)$$

where \hat{v} is the diagonal matrix of channel velocities v_n . Together with Eq. (3) this equation defines the LDOS via the reflection matrices.

In the case of uncorrelated disorder the reflection matrices r_L and r_R are statistically independent, which makes Eq. (10) useful for practical calculations.

In general the LDOS oscillates on the scale of λ_F (due to the prevailing contribution of one particular quantum state). These Friedel-type oscillations can play a crucial role especially in one dimension. In what follows we are concerned with the smoothed version of the LDOS that does not change on the scale of the Fermi wave length and, therefore, also not in the transversal direction. For this purpose we introduce the spatially averaged LDOS

$$n(x, \varepsilon) = \delta V^{-1} \int_{\delta V} n(\vec{r}, \varepsilon) d\vec{r}, \quad (11)$$

where the integration is carried out over a volume δV around the point $(x, \vec{\rho})$. The linear size of the volume δV is assumed to be much larger than the Fermi wave

length and much smaller than the mean free path ℓ . For $|x - x'| \ll \ell$ the reflection matrices defined at the cross section x' are related to those defined at x by

$$r_L(x') = e^{-i\hat{k}(x-x')} r_L(x) e^{-i\hat{k}(x-x')}, \quad (12a)$$

$$r_R(x') = e^{i\hat{k}(x-x')} r_R(x) e^{i\hat{k}(x-x')}, \quad (12b)$$

with $\hat{k} = m_e \hat{v}$. Expanding the right-hand side of Eq. (10) in a geometric series in r_L, r_R we notice that only the terms with equal numbers of r_L and r_R matrices do not oscillate on the scale of the Fermi wave length and have to be kept. Additionally the averaging in the transversal direction mixes up the different modes so that $\langle m | \vec{\rho} \rangle \langle \vec{\rho} | n \rangle \propto \delta_{mn}$ in Eq. (3). As the result we obtain

$$n(x, \varepsilon) = \frac{n_0}{N} \operatorname{Re} \operatorname{Tr} \frac{1 + r_R r_L}{1 - r_R r_L}, \quad (13)$$

where n_0 is the bulk value of the LDOS in the normal metal, which is set to unity in the rest of the paper. In what follows we apply Eq. (13) to calculate the LDOS in the normal-metal wire in the immediate vicinity of an NS interface.

III. LDOS NEAR THE IDEAL NS INTERFACE

The relation (13) applies straightforwardly to the model of the NS junction discussed in the Introduction. The only modification is the doubling of size of the reflection matrices due to particle-hole conversion. We still denote the number of electron channels in the wire by N , so that the size of the particle-hole reflection matrix is now $2N$. Equation (13) can be written in the form

$$n(x, \varepsilon) = 1 + \frac{2}{2N} \operatorname{Re} \operatorname{Tr} \sum_{n=1}^{\infty} (r_L r_R)^n, \quad (14)$$

where r_L is the electron-hole reflection matrix for the long normal-metal wire, while r_R is that for the ideal NS interface. These reflection matrices are conveniently parametrised by

$$r_L = \begin{pmatrix} r_0(\varepsilon) & 0 \\ 0 & r_0(-\varepsilon)^* \end{pmatrix}, \quad r_R = e^{-i\phi_A} \begin{pmatrix} 0 & 1 \\ 1 & 0 \end{pmatrix}, \quad (15)$$

where $\phi_A = \arccos \varepsilon / \Delta$ is the Andreev phase and $r_0(\varepsilon)$ [$r_0(\varepsilon)^*$] is $N \times N$ reflection matrix of the electron-like [hole-like] quasiparticles for the normal-metal wire. The matrix product $r_L r_R$ is block off-diagonal, hence only the even powers n contribute to the trace in Eq. (14). From Eqs. (14,15) we obtain

$$n(x, \varepsilon) = 1 + \frac{2}{N} \operatorname{Re} \operatorname{Tr} \sum_{n=1}^{\infty} [r_0(\varepsilon) r_0(-\varepsilon)^*]^n e^{-2i n \phi_A}. \quad (16)$$

The right-hand side of Eq. (16) is completely determined by the eigenvalues of the correlator $r_0(\varepsilon) r_0(-\varepsilon)^*$,

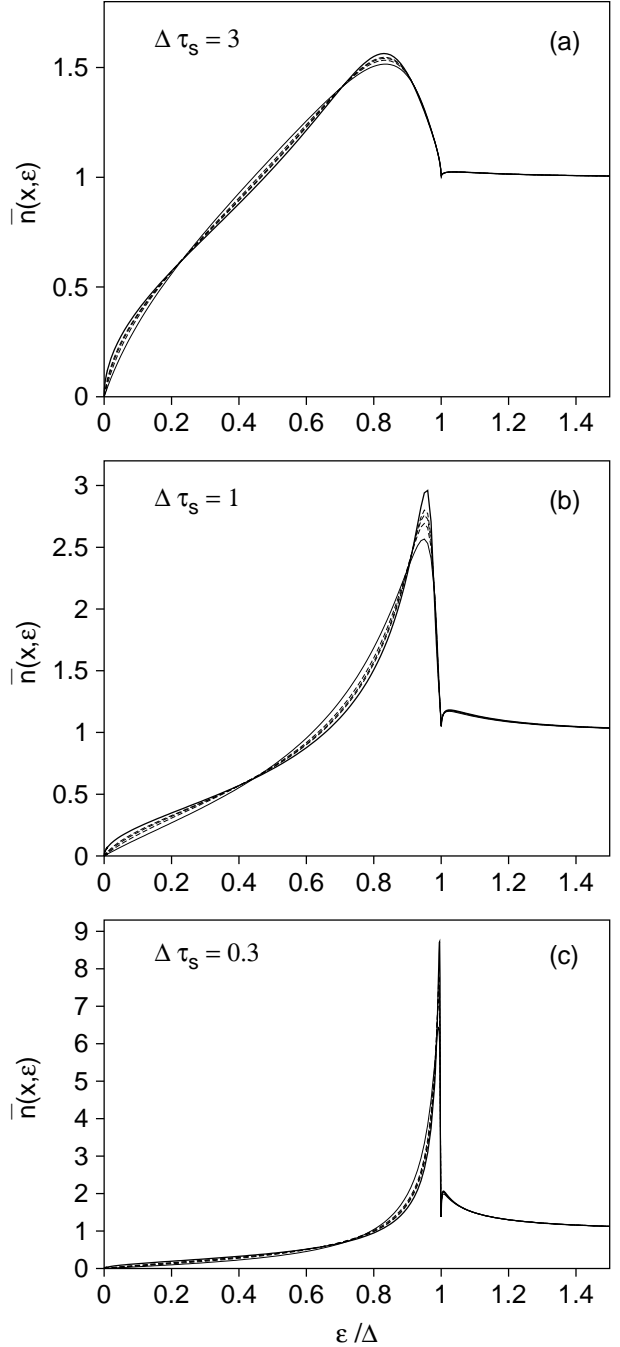


FIG. 2. The mean LDOS (25) in an N -channel normal-metal wire in the immediate neighbourhood of an ideally transmitting NS interface. The curves are calculated from Eqs. (24,25). The thick (thin) solid line corresponds to the limiting case of the multi(single)-channel wire. The dashed lines are for the finite number of channels $N = 2, 3$, and 4 . The figures correspond to the clean regime $\Delta\tau_s = 3$ (top), the intermediate regime $\Delta\tau_s = 1$ (middle), and the dirty regime $\Delta\tau_s = 0.3$ (bottom).

which is a unitary matrix. Its eigenvalues are conveniently parametrised by $\exp(2i\phi_j)$, $j = 1, 2, \dots, N$, where the phases ϕ_j are restricted to the interval $(0, \pi)$. The joint probability density $P_\varepsilon(\phi_1, \phi_2, \dots, \phi_N)$ is a symmetric function with respect to any permutation of its arguments because of the statistical equivalence of the channels. This function has been studied in detail in Ref. 19. Our calculation is restricted to the mean LDOS $\bar{n}(x, \varepsilon) \equiv \langle n(x, \varepsilon) \rangle$, where the angular brackets correspond to the average over the disorder potential in the wire. In order to perform the average in Eq. (16), it is enough to know only the probability density $\rho_\varepsilon(\phi)$ of a single eigenphase. It is instructive to compare Eq. (16) with the similar representation of the integrated density of states in the case of the normal-metal wire of finite length, which has been analysed recently.²⁶

When the Andreev phase ϕ_A is real, i.e., for $\varepsilon < \Delta$, the mean LDOS is found from Eq. (16) as

$$\bar{n}(x, \varepsilon) = \pi \rho_\varepsilon(\phi_A), \quad \varepsilon < \Delta, \quad (17)$$

where the eigenphase density $\rho_\varepsilon(\phi)$ is assumed to be normalised to unity on the interval $(0, \pi)$. The probability density $\rho_\varepsilon(\phi)$ acquires its simplest form in the case $N \gg 1$ of a large number of channels¹⁹,

$$\rho_\varepsilon(\phi) = \frac{1}{\pi \sin^2 \phi} \operatorname{Im} \sqrt{(\varepsilon \tau_s)^2 + i \varepsilon \tau_s (1 - e^{-2i\phi})}, \quad (18)$$

and in the single-channel case^{27,28},

$$\rho_\varepsilon(\phi) = \frac{\varepsilon \tau_s}{\pi} \int_0^\infty \frac{\exp(-\varepsilon \tau_s t)}{t^2 \sin^2 \phi - t \sin 2\phi + 1} dt. \quad (19)$$

The scattering time τ_s of the DMPK scaling equation differs by a numerical factor (dependent on the dimensionality d of the Fermi surface) from the mean scattering time of the transport theory τ'_s . Namely, $\tau_s = c_d \tau'_s$, where $c_d = 2, \pi^2/4, 8/3$, for the dimensionality $d = 1, 2, 3$, correspondingly.

Note, that the integrated density of states (DOS) $\nu = L^{-1} \int_0^L \bar{n}(x, \varepsilon) dx$ in the infinite disordered wire $L \rightarrow \infty$ is given by the relation²⁹ $\nu = \pi(\partial/\partial\varepsilon)[\varepsilon \rho_\varepsilon(0)]$, which is similar in spirit to Eq. (17). For wires with on-site disorder (in standard universality classes) the value of $\pi \rho_\varepsilon(0)$ equals to unity irrespective of energy ε ; however it can have a singularity at $\varepsilon = 0$ for wires with a specific disorder symmetry.

So far we were only concerned with the mean LDOS for $\varepsilon < \Delta$. However, the result (17) can be easily extended to the energies above the pair potential value with the help of the analytical continuation $\varepsilon = i\omega$. On the other hand the analytical continuation has another crucial advantage. It transforms the dynamical correlator $r_0(\varepsilon)r_0(-\varepsilon)^*$ into the essentially static object $r_0(i\omega)r_0(i\omega)^*$. In the absence of a magnetic field the time-reversal symmetry is preserved and the reflection matrix r_0 is symmetric, hence $r_0(i\omega)^* = r_0(i\omega)^\dagger$.

The eigenvalues $\exp(2i\phi_j)$ of the matrix $r_0(\varepsilon)r_0(-\varepsilon)^*$ are transformed to the real eigenvalues R_j of the matrix $r_0(i\omega)r_0(i\omega)^*$, which are the probabilities of the reflection from the long disordered wire in the presence of a spatially uniform fictitious absorption ω .

The summation in Eq. (14) is performed in terms of the eigenvalues

$$n(x, \varepsilon) = \frac{1}{N} \operatorname{Re} \sum_{j=1}^N \frac{1 - R_j \alpha^2(\omega)}{1 + R_j \alpha^2(\omega)} \Bigg|_{\omega=-i\varepsilon+0^+}, \quad (20)$$

where 0^+ is an infinitesimally small positive imaginary part of energy which ensures the retarded Green function required in Eq. (3). We have also introduced

$$\alpha(\omega) = ie^{-i\phi_A} = \sqrt{1 + (\omega/\Delta)^2} - \omega/\Delta. \quad (21)$$

The joint probability density of the eigenvalues R_j for the infinitely long wire is given by the stationary solution of the DMPK equation. In the parametrisation

$$R_j = \frac{\sigma_j}{\sigma_j + 2(N+1)\omega\tau_s}, \quad \sigma_j \in (0, \infty), \quad (22)$$

this solution takes the simple form

$$P(\{\sigma_j\}) = c_N \prod_{j=1}^N e^{-\sigma_j/4} \prod_{k>j} |\sigma_k - \sigma_j|, \quad (23)$$

which we recognise as the orthogonal Laguerre ensemble of random matrix theory³⁰ (with normalisation constant c_N). This ensemble corresponds to the class *CI* in the classification scheme of Ref. 31. The probability density (one-point function) $\rho(\sigma)$, normalized to unity in the interval $(0, \infty)$, is given by³²

$$\rho(\sigma) = \frac{e^{-\sigma}}{N} \left(\sum_{n=0}^{N-1} [L_n^{(0)}(\sigma)]^2 - \frac{1}{2} L_{N-1}^{(0)}(\sigma) L_{N-1}^{(1)}(\sigma) \right. \\ \left. + \frac{1}{4} L_{N-1}^{(1)}(\sigma) \int_0^\sigma d\zeta e^{(\sigma-\zeta)/2} L_{N-1}^{(0)}(\zeta) \right), \quad (24)$$

where $L_n^{(p)}(\sigma)$ is the generalised Laguerre polynomial.

We substitute the parametrisation (22) in Eq. (20) and average over disorder with the help of the density $P(\{\sigma\})$. The result reads

$$\bar{n}(x, \varepsilon) = \operatorname{Re} \int_0^\infty d\sigma \rho(\sigma) \frac{1 - \frac{\alpha^2(\omega)-1}{2(N+1)\omega\tau_s} \sigma}{1 + \frac{\alpha^2(\omega)+1}{2(N+1)\omega\tau_s} \sigma} \Bigg|_{\omega=-i\varepsilon+0^+}. \quad (25)$$

This equation extends Eq. (17) to energies larger than Δ . It can also be applied for arbitrary N . In the large- N limit the distribution $\rho(\sigma)$ can be approximated by³²

$$\lim_{N \rightarrow \infty} N \rho(\zeta N) = \frac{1}{2\pi} \sqrt{\frac{4}{\zeta} - 1}. \quad 0 < \zeta < 4. \quad (26)$$

Substituting this expression into Eq. (25) we reproduce the results of Eqs. (17,18) for $\varepsilon < \Delta$. In the limit $\varepsilon \rightarrow 0$ this leads to the square root behavior of the LDOS $\bar{n}(x, \varepsilon \rightarrow 0) = \text{Re} \sqrt{i\varepsilon}$.

However the Thouless energy $\varepsilon_c = 1/N^2\tau_s$ remains unresolved within the multi-channel approximation (26). In order to fix the scale ε_c one has to take advantage of another limiting relation³³

$$\lim_{N \rightarrow \infty} \rho(\zeta/N) = J_1^2(2\sqrt{\zeta}) - J_0(2\sqrt{\zeta})J_2(2\sqrt{\zeta}) + (2\sqrt{\zeta})^{-1} J_0(2\sqrt{\zeta})J_1(2\sqrt{\zeta}), \quad (27)$$

where J_n are Bessel functions. In the limit $\varepsilon \rightarrow 0$ one can safely put $\alpha(\omega) = 1$ in Eq. (25) and take the real part explicitly,

$$\bar{n}(x, \varepsilon) = \int_0^\infty d\sigma \rho(\sigma) \frac{1}{1 + \sigma^2[(N+1)\varepsilon\tau_s]^{-1}}. \quad (28)$$

To leading order in $\varepsilon/\varepsilon_c$ the function $\rho(\sigma)$ in (28) can be approximated by its value at the origin $\rho(0) = 1/2$, which holds for $\sigma \ll N^{-1}$ [see Eq. (27)]. We therefore obtain

$$\bar{n}(x, \varepsilon) = \frac{\pi(N+1)}{4} \varepsilon \tau_s \approx \frac{\pi}{4N} (\varepsilon/\varepsilon_c), \quad \varepsilon \ll \varepsilon_c. \quad (29)$$

The factor $1/N$ in the last expression reflects the fact that only a single channel is responsible for the non-vanishing LDOS at energies lower than ε_c .

In Fig. 2 we plot the mean LDOS given by Eq. (25) against the ratio ε/Δ for different numbers of channels in the moderately dirty regime $\Delta\tau_s = 0.3$, the intermediate regime $\Delta\tau_s = 1$, and the moderately clean regime $\Delta\tau_s = 3$. We observe that the curves are lying close to each other in all cases. (This suggests that the LDOS near the ideally transmitting interface is quite insensitive to phase-coherent effects.) The situation changes in the case of a finite transparency $\Gamma < 1$ of the NS interface.

IV. EFFECT OF A TUNNEL BARRIER

A. Model

We now introduce the simplest model of a dielectric tunnel barrier at the ideal NS interface. The mean LDOS is calculated in the normal-metal at a ballistic distance $x \ll \ell$ from the interface (see Fig. 1).

We describe the segment I of the wire between the chosen cross section and the ideal NS interface (this segment includes the tunnel barrier) by its S -matrix

$$S_I = \begin{pmatrix} r_1^I & t_2^I \\ t_1^I & r_2^I \end{pmatrix}, \quad (30)$$

where each block itself consists of block-diagonal matrices in the particle-hole representation,

$$r_{1,2}^I = \begin{pmatrix} r_{1,2}(\varepsilon) & 0 \\ 0 & r_{1,2}(-\varepsilon)^* \end{pmatrix}, \quad (31a)$$

$$t_{1,2}^I = \begin{pmatrix} t_{1,2}(\varepsilon) & 0 \\ 0 & t_{1,2}(-\varepsilon)^* \end{pmatrix}, \quad (31b)$$

and the matrices $r_{1,2}(\varepsilon)$, $t_{1,2}(\varepsilon)$ are $N \times N$ electron reflection and transmission matrices corresponding to the segment I .

The right matrix r_R in the fundamental formula (14) depends on the S -matrix of the segment I [see Eqs. (30,31)] and on the scattering matrix for Andreev reflection [see Eq. (15)]. A straightforward algebraic calculation gives²⁰

$$r_R = \begin{pmatrix} r_c(\varepsilon) & -t_c(-\varepsilon)^* \\ t_c(\varepsilon) & r_c(-\varepsilon)^* \end{pmatrix}, \quad (32a)$$

$$t_c(\varepsilon) = e^{-i\phi_A(\varepsilon)} t_2(-\varepsilon)^* M(\varepsilon) t_1(\varepsilon), \quad (32b)$$

$$r_c(\varepsilon) = r_1(\varepsilon) + e^{-2i\phi_A(\varepsilon)} t_2(\varepsilon) r_2(-\varepsilon)^* M(\varepsilon) t_1(\varepsilon), \quad (32c)$$

$$M(\varepsilon) = \left[1 - e^{-2i\phi_A(\varepsilon)} r_2(\varepsilon) r_2(-\varepsilon)^* \right]^{-1}. \quad (32d)$$

In general, if the segment I contains some weak disorder (which is the case, for example, for $x > \ell$) the correlations between the matrices $r_{1,2}$ and $t_{1,2}$ for electron- and hole-like quasiparticles are non-trivial. We consider here the case that the segment I contains no disorder, but a sufficiently steep tunnel barrier which makes no difference in the tunnelling probability of electrons and holes. In this case we can omit the energy dependence in the matrices $r_{1,2}$ and $t_{1,2}$. In what follows we take advantage of the polar decomposition

$$\begin{pmatrix} r_1 & t_2 \\ t_1 & r_2 \end{pmatrix} = \begin{pmatrix} u_I & 0 \\ 0 & v_I^T \end{pmatrix} \begin{pmatrix} \sqrt{1-\Gamma} & i\sqrt{\Gamma} \\ i\sqrt{\Gamma} & \sqrt{1-\Gamma} \end{pmatrix} \begin{pmatrix} u_I^T & 0 \\ 0 & v_I \end{pmatrix} \quad (33)$$

where u_I , v_I are some unitary matrices, which depend on a particular realisation of the barrier, and Γ is the diagonal matrix of the tunnelling probabilities Γ_j . Time-reversal symmetry in the segment I is assumed. Once the dependence on energy in the matrices u_I , v_I and Γ is disregarded we obtain from Eqs. (32,33) the right reflection matrix

$$r_R = \begin{pmatrix} u_I & 0 \\ 0 & u_I^* \end{pmatrix} \begin{pmatrix} e^{i\chi} \cos \theta & -ie^{i\chi} \sin \theta \\ -ie^{i\chi} \sin \theta & e^{i\chi} \cos \theta \end{pmatrix} \begin{pmatrix} u_I^T & 0 \\ 0 & u_I^\dagger \end{pmatrix}, \quad (34a)$$

$$\sin \theta = \Gamma [(1 - e^{2i\phi_A}(1 - \Gamma))(1 - e^{-2i\phi_A}(1 - \Gamma))]^{-\frac{1}{2}}, \quad (34b)$$

$$e^{2i\chi} = (1 - \Gamma - e^{2i\phi_A}) [1 - e^{2i\phi_A}(1 - \Gamma)]^{-1}. \quad (34c)$$

The left matrix r_L is given by Eq. (15) and describes the reflection from the disordered wire. Taking advantage of the polar decomposition we can write

$$r_L = \begin{pmatrix} u_0 & 0 \\ 0 & u_0^* \end{pmatrix} \begin{pmatrix} e^{i\phi} & 0 \\ 0 & e^{i\phi} \end{pmatrix} \begin{pmatrix} u_0^T & 0 \\ 0 & u_0^\dagger \end{pmatrix} \quad (35)$$

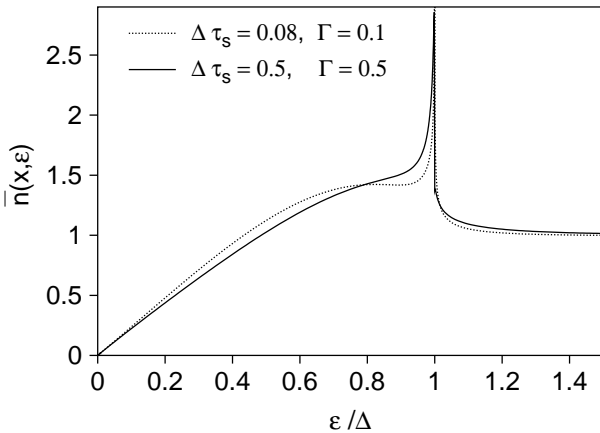


FIG. 3. The mean LDOS (40) in a single-channel disordered wire at ballistic distance from a NS interface of finite transparency. The parameters $\Delta\tau_s = 0.5, \Gamma = 0.5$ (solid line) and $\Delta\tau_s = 0.08, \Gamma = 0.1$ (dashed line) are chosen to keep the combination $\Delta\tau_s(2 - \Gamma)/\Gamma$ fixed. The curves are close to each other for $\varepsilon \ll \Delta$ where Eq. (38) is applicable.

where u_0 is a random unitary matrix and ϕ is the diagonal matrix of the eigenphases. We see that all information contained in u_I disappears statistically from the eigenvalues of $r_L r_R$ because the product $u_I^T u_0$ can be regarded again as a random unitary matrix. Thus the disorder-averaged LDOS depends only on the transmission eigenvalues Γ_j of the tunnel barrier. Below we calculate the mean LDOS for a single-channel wire and for a multi-channel wire provided the tunnelling probabilities are the same for all channels, i.e., $\Gamma_j = \Gamma$.

B. Single channel wire

We start with the calculation of the mean LDOS for $\varepsilon < \Delta$ in the case of the single-channel wire $N = 1$. For $\varepsilon < \Delta$ the phases χ and θ defined in Eq. (34) are real and both r_L and r_R are unitary 2×2 matrices. We denote $u_I^T u_0 = \exp(i\psi)$, where ψ is a random phase distributed uniformly in the interval $(0, 2\pi)$. We insert the reflection matrices from Eqs. (34a,35) directly to Eq. (13). The matrix $(1 - r_L r_R)$ can be easily inverted. Taking the real part we notice that the zeroes of $\text{Det}(1 - r_L r_R)$ define the exact positions of the quasiparticle bound states for $\varepsilon < \Delta$. The result reads

$$n(x, \varepsilon) = \pi \sin(\phi + \chi) \delta(\cos \theta \cos \psi - \cos(\phi + \chi)), \quad (36)$$

where the argument of the Dirac δ -function corresponds to the quantisation condition for the bound states. The mean LDOS is given by the average over the phase ϕ with the probability density $\rho_\varepsilon(\phi)$ of Eq. (19), and over the uniformly distributed phase ψ . The integration over ψ is readily done with the result

$$\bar{n}(x, \varepsilon) = \int_{\theta-\chi}^{\pi-\theta-\chi} d\phi \rho_\varepsilon(\phi) \frac{\sin(\phi + \chi)}{\sqrt{\cos^2 \theta - \cos^2(\phi + \chi)}}. \quad (37)$$

In the limit $\Gamma \rightarrow 1$ of the vanishing tunnel barrier one observes that $\chi \rightarrow \pi/2 - \phi_A$ and $\theta \rightarrow \pi/2$, so that the area of the integration in Eq. (36) shrinks to the small vicinity of $\phi = \phi_A$ and the function $\rho_\varepsilon(\phi)$ can be substituted by its value in this point. The integral approaches π and we recover the result of Eq. (17) for the ideally transmitting interface.

In the opposite extreme of a high tunnel barrier ($\Gamma \rightarrow 0$) both θ and χ go to zero, so that the integration area is not restricted and the value of the integral tends to unity because of the normalisation condition for the probability density $\rho_\varepsilon(\phi)$. In the limit $\varepsilon \ll \Delta$ we can set $\chi = 0$ and reduce Eq. (37) to the following form

$$\bar{n}(x, \varepsilon) = \text{Re} \int_0^\infty dt e^{-t} \left[1 - \frac{\sin^2 \theta}{(\varepsilon \tau_s)^2} t(t - 2i\varepsilon \tau_s) \right]^{-\frac{1}{2}}, \quad (38)$$

where $\sin \theta = \Gamma/(2 - \Gamma)$, according to Eq. (34b). From Eq. (38) we find that

$$\bar{n}(x, \varepsilon) = \pi \varepsilon \tau_s \frac{2 - \Gamma}{2\Gamma}, \quad \varepsilon \tau_s \ll \frac{\Gamma}{2 - \Gamma}, \quad (39)$$

which coincides for $\Gamma = 1$ with the result of Eq. (29) for $N = 1$. In the dirty limit $\Delta \ll \tau_s^{-1}$ and for a high tunnel barrier $\Gamma \ll 1$ the result of Eq. (38) is applicable almost up to the value of $\varepsilon = \Delta$. It describes the formation of the pseudo-gap near the energy $\tau_s^{-1}\Gamma$ due to the normal reflection from the barrier.

The exact expression (37) additionally accounts for the peak at $\varepsilon \simeq \Delta$. This expression can be further generalised for energies higher than Δ by means of the analytical continuation $\varepsilon = i\omega$, with the result

$$\bar{n}(x, \varepsilon) = -\text{Re} \int_0^\infty d\sigma \rho_1(\sigma) \frac{\sinh Q(\sigma)}{\sqrt{\sinh^2 Q(\sigma) + \sin^2 \theta}}, \quad (40a)$$

$$Q(\sigma) = \frac{1}{2} \ln \frac{\alpha^2(\omega) + 1 - \Gamma}{1 + \alpha^2(\omega)(1 - \Gamma)} + \frac{1}{2} \ln \frac{\sigma}{\sigma + 4\omega \tau_s}, \quad (40b)$$

where the function $\rho_1(\sigma) = (1/2) \exp(-\sigma/2)$ is the probability density (24) for a single-channel wire, the function $\alpha(\omega)$ is defined in Eq. (21), and the continuation to the real energies $\omega \rightarrow -i\varepsilon + 0^+$ is performed.

C. Multi-channel wire

The disorder-averaged LDOS for $N \gg 1$ can be found straightforwardly for the case of equivalent tunnelling probabilities $\Gamma_j = \Gamma$. Then the diagonal matrices θ and χ in Eqs. (34b,34c) can be regarded as scalars. It is convenient to make use of the analytical continuation $\varepsilon = i\omega$ and define

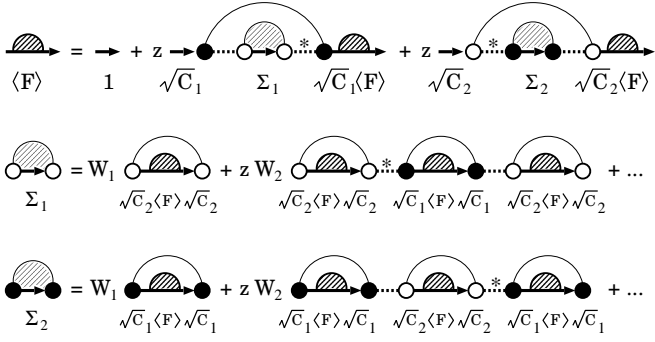


FIG. 4. Diagrammatic representation of the Dyson equation (46) for $\langle F(z) \rangle_U$.

$$\alpha(\omega) = ie^{i\phi_A}, \quad R = e^{2i\phi}, \quad (41a)$$

$$p = e^{2i\chi} = \frac{\alpha^2(\omega) + 1 - \Gamma}{1 + \alpha^2(\omega)(1 - \Gamma)}, \quad (41b)$$

where $R = \text{diag}(R_1, \dots, R_N)$ is the diagonal matrix of reflection probabilities for the disordered wire with a fictitious absorption ω . In the parametrisation (22) the joint probability density of R_j is related to the orthogonal Laguerre ensemble (23). Note that the quantities p , R_j and $\alpha(\omega)$ take real values in the interval $(0, 1)$ when ω is real.

The basic expression (14) for the mean LDOS is manifestly invariant under an arbitrary unitary rotation of the matrix product $r_L r_R$. From Eqs. (34a,35) we obtain

$$U_0^\dagger r_L r_R U_0 = \begin{pmatrix} \sqrt{pR} & 0 \\ 0 & \sqrt{pR} \end{pmatrix} \begin{pmatrix} \cos \theta & -i \sin \theta \\ -i \sin \theta & \cos \theta \end{pmatrix} U^\dagger, \quad (42a)$$

$$U = u_0^T u_I u_I^T u_0, \quad U_0 = \text{diag}(u_0, u_0^*), \quad (42b)$$

where we take advantage of the quantities defined in Eq. (41). The matrix u_0 is a random unitary matrix which is uniformly distributed in the unitary group (provided the weak disorder $k_F \ell \gg 1$). Hence by construction (42b) U is the unitary symmetric random matrix. We substitute Eq. (42a) into Eq. (14) to express the mean LDOS as

$$\bar{n}(x, \varepsilon) = \frac{1}{N} \text{Re} \text{Tr} \left\langle \frac{1 - pR}{1 + pR} \langle F(\cos \theta) \rangle_U \right\rangle_R, \quad (43)$$

where

$$F(z) = \frac{1}{1 - z(\sqrt{C_1} U \sqrt{C_2} + \sqrt{C_2} U^\dagger \sqrt{C_1})}, \quad (44a)$$

$$C_1 = \frac{pR}{1 + pR}, \quad C_2 = \frac{1}{1 + pR}. \quad (44b)$$

The average over disorder in Eq. (43) is decoupled into two independent steps: the average $\langle \dots \rangle_U$ over the group spanned by the unitary symmetric matrices and the average $\langle \dots \rangle_R$ over the orthogonal Laguerre ensemble of the reflection eigenvalues R_j .

In the case of the finite number of channels the calculation of average over the unitary matrices U is technically

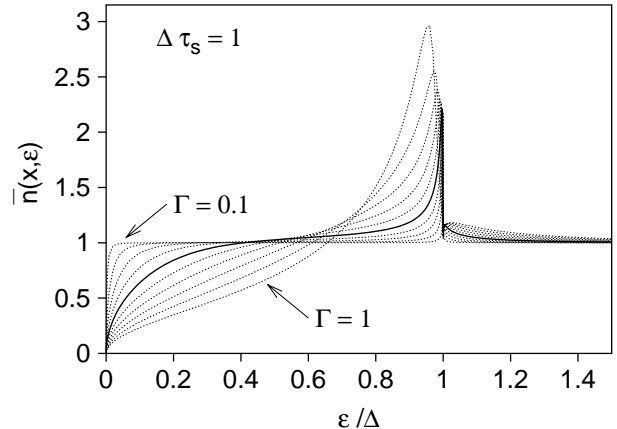


FIG. 5. The mean LDOS in the diffusive normal-metal wire in the vicinity of the NS interface of finite transparency. The curves are calculated from Eqs. (53,56) in the multi-channel limit ($N \gg 1$) provided $\Delta\tau_s = 1$ and the effective tunnelling probability Γ ranges from 0.1 to 1 with the step 0.1. The solid line corresponds to $\Gamma = 0.5$.

difficult and cannot be done analytically. However, for the diffusive wire, $N \gg 1$, the calculation can be done by means of the diagrammatic technique developed in Ref. 34.

Let us briefly quote the basic substitution rules of the diagrammatic technique

$$\begin{aligned} U_{ij} &= \bullet \cdots \circ, & U_{ij}^* &= \bullet \cdots \circ^*, \\ C_{ij} &= \xrightarrow{\text{C}}, & \delta_{ij} &= \text{---}. \end{aligned} \quad (45)$$

Here the matrix element U_{ij} is represented by the black and white dot connected by the dashed line. The black dot stays for the first index i and the white dot for the second index j . The conjugated matrix U^* is marked by a star. The other matrices are denoted by thick solid arrows. The summation over a matrix index in a dot is indicated by the attachment of a solid line. The average over the unitary symmetric matrices is symbolically performed by pairing in all possible ways all black and white dots belonging to U to all black and white dots belonging to U^* . This pairing is denoted by the thin solid line, which corresponds to the Kronecker symbol. The result of the averaging is found by inspection of the closed circuits in the diagram which consist of alternating thick and thin solid lines (T-circles). Each diagram is weighted by a factor, which is obtained by inspection of the closed circuits of alternating thin solid and dashed lines (U-circles).

We expand the matrix $F(z)$ (44) into a geometric series and keep only the terms with equal number of U and U^\dagger matrices. In the large- N limit we have to take into account the diagrams with the largest number of T-circles³⁴. This amounts to the summation of the ‘rainbow’ diagrams, or diffusion ladders, depicted symbolically in Fig. 4. The corresponding Dyson equation is

$$\langle F \rangle_U = \hat{1} + z\Sigma_1 C_1 \langle F \rangle_U + z\Sigma_2 C_2 \langle F \rangle_U, \quad (46a)$$

$$\Sigma_1 = \sum_{n=1}^{\infty} W_n z^{n-1} [\text{Tr } C_2 \langle F \rangle_U]^n [\text{Tr } C_1 \langle F \rangle_U]^{n-1}, \quad (46b)$$

$$\Sigma_2 = \sum_{n=1}^{\infty} W_n z^{n-1} [\text{Tr } C_1 \langle F \rangle_U]^n [\text{Tr } C_2 \langle F \rangle_U]^{n-1}, \quad (46c)$$

where the weight factors

$$W_n = N^{1-2n} (-1)^{n-1} \frac{(2n-2)!}{n!(n-1)!} + \mathcal{O}(N^{-2n}) \quad (47)$$

have been found in Ref. 34. Taking the coefficients W_n to the leading order in N we define the generating function

$$h(s) = \sum_{n=1}^{\infty} W_n s^{n-1} = \frac{1}{2s} \left(\sqrt{N^2 + 4s} - N \right), \quad (48)$$

which may be used to reduce Eq. (46) to

$$\begin{aligned} \langle F(z) \rangle_U &= \hat{1} + z^2 h(z^2 s_1 s_2) (s_1 C_1 + s_2 C_2) \langle F(z) \rangle_U, \\ s_{1,2} &= \text{Tr } C_{1,2} \langle F(z) \rangle_U. \end{aligned} \quad (49)$$

The matrix $\langle F(z) \rangle_U$ can be eliminated from the Dyson equation Eq. (49). It is very convenient to transform to the new scalar variables

$$X = \frac{s_2 - s_1}{N}, \quad Y = \frac{s_2 + s_1}{N}, \quad (50)$$

which obey the equations

$$\frac{X+1}{2} = \frac{1}{N} \text{Tr} \frac{1}{1 + pR f(X, Y)}, \quad (51a)$$

$$Y^2 \sin^2 \theta + X^2 \cos^2 \theta = 1, \quad (51b)$$

with

$$f(X, Y) = \frac{(1-X)(Y+X)}{(1+X)(Y-X)}, \quad (52)$$

where we have substituted $z = \cos \theta$ and the matrices C_1 , C_2 from Eq. (44b).

In terms of the variables X and Y the mean LDOS (43) is simplified to

$$\bar{n}(x, \varepsilon) = \text{Re } \bar{X}(\omega)|_{\omega \rightarrow -i\varepsilon + 0^+}, \quad (53)$$

where the bar stands for the average over the ensemble of the reflection probabilities: $\bar{X} \equiv \langle X \rangle_R$.

Let us consider the case of equal reflection probabilities $R_j = R$. The matrix U in Eq. (44) commutes with C_1 and C_2 and can be diagonalised, hence the problem becomes equivalent to that of a single channel wire. The solution of the self-consistent equations Eq. (51) is given by

$$X = -\frac{\sinh Q}{\sqrt{\sinh^2 Q + \sin^2 \theta}}, \quad Q = \frac{1}{2} \ln pR, \quad (54)$$

which coincides with the result of the exact integration over U . This proves that the set of diagrams which we took into account in Eqs. (46) is complete enough. The substitution of Eq. (54) in Eq. (53) and the additional average over the reflection probability of a single channel wire yields the mean LDOS of Eq. (40).

In the multichannel (diffusive) limit $N \gg 1$ the reflection probabilities R_j are, in fact, not equal. Moreover they effectively repel each other according to Eqs. (22,23). In this case Eq. (51) can no longer be solved in closed form. In other words, the averages over the random matrix U and over the reflection eigenvalues R_j cannot be performed separately.

In order to proceed one has to take advantage of the self-averaging property of the variables X and Y in the limit $N \gg 1$. Indeed both variables are defined via the traces $s_{1,2}$ and can be thought as the arithmetic means of N fluctuating quantities. From physical point of view the variable X is proportional to the one-point Green function, therefore it is self-averaging in a diffusive metal.

Thus we can construct the self-consistent equation for \bar{X} by taking the average over R on both sides of Eq. (51a). We assume a fixed value of $f(X, Y(X)) = \tilde{f}(\bar{X})$ on the right side, neglecting the fluctuations of X . Taking advantage of the square-root approximation (26) of the density $\rho(\sigma)$ we obtain

$$\frac{\bar{X} + 1}{2} = \frac{1}{2\pi} \int_0^4 d\zeta \sqrt{\frac{4}{\zeta} - 1} \frac{2\omega\tau_s + \zeta}{2\omega\tau_s + (1 + p\tilde{f}(\bar{X}))\zeta}. \quad (55)$$

The integral on the right-hand side can be carried out explicitly giving rise to the equation

$$\begin{aligned} &\frac{(\alpha^2(\omega) + 1 - \Gamma)(Y(\bar{X}) + \bar{X})}{(1 + \alpha^2(\omega)(1 - \Gamma))(Y(\bar{X}) - \bar{X})} \\ &= 1 + \frac{2}{1 + \bar{X}} \left(\omega\tau_s - \sqrt{\omega\tau_s} \sqrt{1 + \bar{X} + \omega\tau_s} \right), \end{aligned} \quad (56)$$

which is an algebraic equation for \bar{X} . It can be analytically continued to real energies $\omega = -i\varepsilon + 0^+$ and solved numerically by iteration. The disorder-averaged LDOS is determined, then, from Eq. (53). Equation (56) is obtained in the quasiclassical limit of a large number of channels. This result does not change if we neglect that U is symmetric or take the unitary Laguerre ensemble in Eq. (23) instead of the orthogonal one.

The weak-localisation correction (which we simply define as $1/N$ correction) can, in principle, be determined within the present approach. It has three different sources. First of all an additional class of diagrams, namely the cooperon-like diagrams, have to be taken into account in the Dyson equation (46). Secondly the term of sub-leading order in the large- N expansion of the weight factors W_n has to be included. Finally the correction of order $\mathcal{O}(N^{-1})$ to the limiting form (26) of the probability density $\rho(\sigma)$ has to be considered. The calculation of

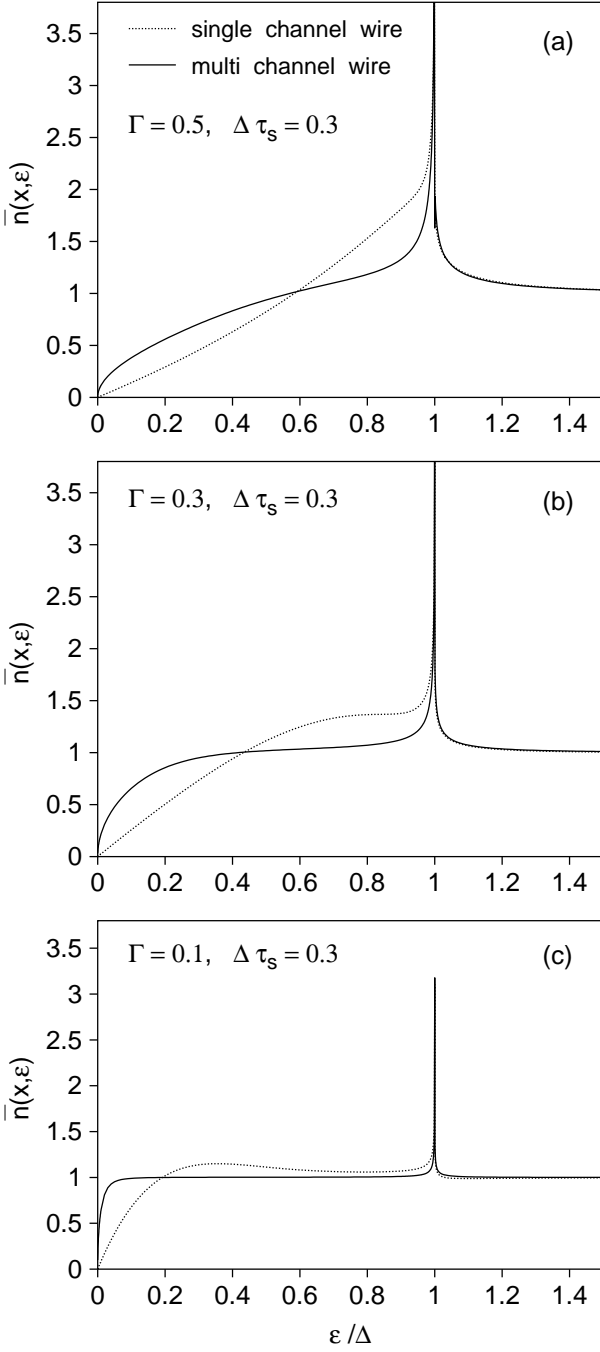


FIG. 6. The mean LDOS in a normal-metal wire in the vicinity of a NS interface of finite transparency. The solid curve is calculated from Eqs. (53,56) for the diffusive wire ($N \gg 1$). The dashed curve is found from Eq. (40) for the single-channel wire ($N = 1$). The ratio $\ell/\xi = \Delta\tau_s = 0.3$ is fixed, which corresponds to the moderately dirty limit. The figures show the dependence of the mean LDOS on the transparency of the interface: $\Gamma = 0.5$ (top), $\Gamma = 0.3$ (middle), and $\Gamma = 0.1$ (bottom).

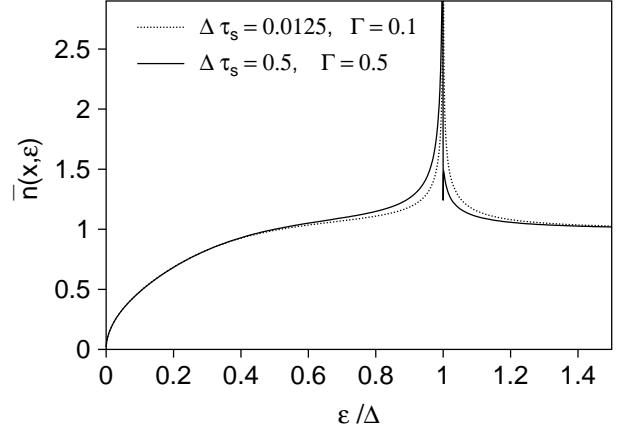


FIG. 7. The mean LDOS in a diffusive disordered wire in the vicinity of a NS interface of finite transparency calculated from Eqs. (53,56). The parameters $\Delta\tau_s = 0.5$, $\Gamma = 0.5$ (solid line) and $\Delta\tau_s = 0.0125$, $\Gamma = 0.1$ (dashed line) are chosen to keep the combination $\Delta\tau_s(2 - \Gamma)^2/\Gamma^2$ fixed. The curves coincide for $\varepsilon \ll \Delta$ where Eq. (59) is applicable.

the weak localisation correction to the LDOS is, however, beyond the scope of this paper.

In some limiting cases Eq. (56) allows for a transparent analytical solution. In the absence of the tunnel barrier $\Gamma = 1$ we obtain

$$\bar{X} = 1 - 2 \frac{\alpha^2}{1 + \alpha^2} \left(1 + \Omega - \sqrt{\Omega} \sqrt{2 + \Omega} \right) \Big|_{\Omega \rightarrow \frac{\omega\tau_s}{1 + \alpha^2}}, \quad (57)$$

which coincides upon the substitution in (53) with the result of Eq. (25) in the large- N limit.

For small energies, $\omega \ll \Delta$, we can put $\alpha(\omega) = 1$ and obtain

$$\bar{X} = \frac{\sqrt{\omega\tau_s} \sqrt{4 \sin^2 \theta + \omega\tau_s - \omega\tau_s}}{2 \sin^2 \theta}. \quad (58)$$

The mean LDOS (53) for $\varepsilon \ll \Delta$ is then given by

$$n(x, \varepsilon) = \text{Re} \sqrt{-i \frac{\varepsilon\tau_s}{\sin^2 \theta}} \sqrt{1 - i \frac{\varepsilon\tau_s}{4 \sin^2 \theta}}, \quad (59)$$

with $\sin \theta = \Gamma/(2 - \Gamma)$. This result describes the scaling $\varepsilon_g \sim \tau_s^{-1} \Gamma^2 (2 - \Gamma)^{-2}$ of the size of the pseudogap ε_g with the transparency of the tunnel barrier Γ , which is illustrated in Fig. 7. We observe that in the limit $\tau_s^{-1} \Gamma^2 \ll \Delta \ll \tau_s^{-1}$ two different types of bound states contribute to the LDOS at energies below Δ . One group of the bound states is responsible for the monotonous increase of the LDOS to its bulk value at the scale $\tau_s^{-1} \Gamma^2$ while another group gives rise to the formation of the peak near $\varepsilon = \Delta$.

In our calculation we take the superconducting order parameter to behave like a step function across the NS interface. However the self-consistent treatment of the

order parameter can only modify the energy dependence of the LDOS near $\varepsilon = \Delta$ leaving the monotonous behavior given by Eq. (59) unchanged.

V. CONCLUSION

In conclusion, we compute the mean LDOS in a normal-metal disordered wire in the immediate vicinity of an NS interface at zero temperature and zero magnetic field. Our calculation is based on the scattering approach and takes into account the spatial phase coherence in the normal-metal. The scattering from the superconductor is described within the simple model of Andreev reflection with the order parameter vanishing abruptly to zero in the normal-metal side of NS interface. In our calculation we also disregard any inelastic processes.

We derive the general formula (10), which expresses the one-point Green function in terms of the reflection matrices. The formula can be applied in order to calculate the LDOS (and its distribution) in the normal-metal wire at arbitrary distance to the NS interface. In this paper we only consider the mean LDOS at the ballistic distance to the interface.

We obtain the relation (1) between the disorder-averaged LDOS near the ideal NS interface and the probability density of the eigenphases of the matrix correlator $r_0(\varepsilon)r_0(-\varepsilon)^\dagger$, where $r_0(\varepsilon)$ is the reflection matrix for the semi-infinite normal-metal wire.

We also study in detail the case of the normal-superconductor tunnel junction and derive the self-consistent equation (56) that determines the LDOS in the diffusive normal metal. The semiclassical analysis of the Green function at the NS interface of finite transparency has been performed by many authors^{35–38} in connection with the boundary conditions of semiclassical superconductivity. However, to our best knowledge there exists no counterpart to the equation (56) in the literature.

The effect of Anderson localisation is seen in the linear increase of the LDOS for the energies lower than $\varepsilon_c = \hbar/N^2\tau_s$. In the diffusive metal, $N \rightarrow \infty$, the LDOS increases as the square root of energy. The form of the crossover in the energy dependence of the LDOS from linear to square root behavior is given by Eq. (25) for weak disorder and perfect NS interface.

ACKNOWLEDGMENTS

We thank C. W. J. Beenakker, P. W. Brouwer and R. Narayanan for valuable discussions.

- ¹ L. N. Cooper, Phys. Rev. Lett. **6**, 689 (1961).
- ² G. Deutscher and P. G. de Gennes, in *Superconductivity*, edited by R. D. Parks, Vol. 2, p. 1005 (Dekker, New York, 1969).
- ³ *Mesoscopic Electron Transport*, edited by L. P. Kouwenhoven, G. Schön, and L. L. Sohn, NATO ASI Series E, Vol. 345 (Kluwer Academic Publishers, Dordrecht, 1997).
- ⁴ A. F. Andreev, Zh. Eksp. Teor. Fiz. **46**, 1823 (1964) [Sov. Phys. JETP **19**, 1228 (1964)].
- ⁵ F. S. Bergeret, A. F. Volkov, and K. B. Efetov, Phys. Rev. B, **65**, 134505 (2002); K. Halterman and O. T. Valls, Phys. Rev. B, **65**, 014509 (2001); I. Baladié and A. Buzdin, Phys. Rev. B, **64**, 224514 (2001), R. Fazio and C. Lucheroni, Europhys. Lett., **45**, 707 (1999).
- ⁶ M. A. Sillanpää, T. T. Heikkilä, R. K. Lindell, and P. J. Hakonen, Europhys. Lett., **56**, 590 (2001).
- ⁷ N. Moussy, H. Courtois, and B. Pannetier, Europhys. Lett., **55**, 861 (2001).
- ⁸ M. Vinet, C. Chapelier, and F. Lefloch, Phys. Rev. B, **63**, 165420 (2001).
- ⁹ S. Guéron, H. Pothier, N. O. Birge, D. Esteve, and M. H. Devoret, Phys. Rev. Lett., **77**, 3025 (1996).
- ¹⁰ S. H. Tessmer, D. J. Van Harlingen, and J. W. Lyding, Phys. Rev. Lett., **70**, 3135 (1993); S. H. Tessmer, M. B. Tarlie, D. J. Van Harlingen, D. L. Maslov, and P. M. Goldbart, *ibid.* **77**, 924 (1996).
- ¹¹ Y. Levi, O. Millo, N. D. Rizzo, D. E. Prober and L. R. Motowidlo, Phys. Rev. B **58**, 15128 (1998).
- ¹² M. Schechter, Y. Imry, and Y. Levinson, Phys. Rev. B **64**, 224513 (2001).
- ¹³ Ya. V. Fominov and M. V. Feigelman, Phys. Rev. B, **63**, 094518 (2001).
- ¹⁴ S. Pilgram, W. Belzig, C. Bruder, Physica B, **280**, 442 (2000); Phys. Rev. B, **62**, 12462 (2000).
- ¹⁵ W. Belzig, C. Bruder, and G. Schön, Phys. Rev. B, **54**, 9443 (1996).
- ¹⁶ K. D. Usadel, Phys. Rev. Lett., **25**, 507 (1970).
- ¹⁷ G. Eilenberger, Z. Phys., **214**, 195 (1968).
- ¹⁸ K. K. Likharev, Rev. Mod. Phys., **51**, 101 (1979).
- ¹⁹ M. Titov and C. W. J. Beenakker, Phys. Rev. Lett. **85**, 3388 (2000).
- ²⁰ C. W. J. Beenakker, Rev. Mod. Phys. **69**, 731 (1997).
- ²¹ O. N. Dorokhov, Pis'ma Zh. Eksp. Teor. Fiz. **36**, 259 (1982) [JETP Lett. **36**, 318].
- ²² P. A. Mello, P. Pereyra, and N. Kumar, Ann. Phys. (N.Y.) **181**, 290.
- ²³ H. Schomerus, M. Titov, P. W. Brouwer, and C. W. J. Beenakker, Phys. Rev. B **65**, 121101(R) (2002).
- ²⁴ D. S. Fisher and P. A. Lee, Phys. Rev. B **23**, 6851 (1981).
- ²⁵ V. Gasparian, T. Christen, and M. Büttiker, Phys. Rev. A **54**, 4022 (1996).
- ²⁶ M. Titov, N. A. Mortensen, H. Schomerus, and C. W. J. Beenakker, Phys. Rev. B, **64**, 134206 (2001).
- ²⁷ V. L. Berezinskii and L. P. Gor'kov, Sov. Phys. JETP **50**, 1209 (1979).
- ²⁸ B. White, P. Sheng, Z. Q. Zhang, and C. Papanicolaou, Phys. Rev. Lett. **59**, 1918 (1987).
- ²⁹ M. Titov, P. W. Brouwer, A. Furusaki, and C. Mudry, Phys. Rev. B **63**, 235318 (2001).
- ³⁰ M. L. Mehta, *Random Matrices* (Academic, New York,

1991).

- ³¹ A. Altland, M. Zirnbauer, Phys. Rev. B **55**, 1142 (1997).
- ³² K. Slevin and T. Nagao, Phys. Rev. B **50**, 2380 (1994).
- ³³ T. Nagao and K. Slevin, J. Math. Phys. **34**, 2317 (1993).
- ³⁴ P. W. Brouwer and C. W. J. Beenakker, J. Math. Phys. **37**, 4904 (1996).
- ³⁵ A. A. Golubov and M. Yu. Kupriyanov, Zh. Eksp. Teor. Fiz. **96**, 1420 (1989) [Sov. Phys. JETP **69**, 805 (1989)].
- ³⁶ M. Yu. Kupriyanov and V. F. Lukichev, Zh. Eksp. Teor. Fiz. **94**, 139 (1988) [Sov. Phys. JETP **67**, 1163 (1988)].
- ³⁷ A. V. Zaitsev, Phys. Lett. A **194**, 315 (1994).
- ³⁸ A. V. Zaitsev, Zh. Eksp. Teor. Fiz. **86**, 1742 (1984) [Sov. Phys. JETP **59**, 1015 (1984)].